Coupling Smoothed Particle Hydrodynamics Method with Finite Element Method for Air-solid Interaction Modelling of Clapping Wing Micro Air Vehicles

Zhang, Yanwei; Wang, Zhonglai; Pereira Castro, Saullo Giovani

DOI
10.1109/ROBIO55434.2022.10011773

Publication date
2022

Document Version
Final published version

Published in
2022 IEEE International Conference on Robotics and Biomimetics, ROBIO 2022

Proceedings of the 2022 IEEE
International Conference on Robotics and Biomimetics
December 5-9, 2022, Xishuangbanna, China

Coupling Smoothed Particle Hydrodynamics Method with Finite Element Method for Air-solid Interaction Modelling of Clapping Wing Micro Air Vehicles*

Yanwei Zhang[1], Zhonglai Wang[1], and Saullo Giovani Pereira Castro[2]

2022 IEEE International Conference on Robotics and Biomimetics (ROBIO) | 978-1-6654-8109-0/22/$31.00 ©2022 IEEE | DOI: 10.1109/ROBIO55434.2022.10011773

***Abstract*— Inspired by natural birds and insects, a flapping wing micro air vehicle with a double fling-clap mechanism is presented to achieve flapping flight. Smoothed particle hydrodynamics model has proven to be successfully applied to implement water cases. This study focuses on the fluid-solid interaction model coupling smoothed particle hydrodynamics method with the finite element method to handle three-dimensional numerical simulations of flexible clapping wings. Additionally, a validation study is carried out to examine the accuracy of our numerical model. Using the proposed model, analysis under a parametric study shows wingspan of the clapping wings is highly correlated with lift, lift/drag, and lift coefficient. This study provides a high-fidelity air-solid interaction model towards flexible clapping wings and a better understanding of the aerodynamic characteristics of clapping wing micro air vehicles.**

I. INTRODUCTION

The development of flapping wing micro air vehicles (FWMAVs) in recent years has been inspired heavily by insects and birds [1], [2]. Flying biomechanics is the primary focus of FWMAV. On the one hand, scientists must know how flapping wing propulsion interacts with biological physiology, ecology, animal behavior, and evolution. On the other hand, designers of FWMAV must be proficient in biomechanical technology to design prototypes. Biomimetics is a rapidly expanding field that requires a variety of theoretical backing. In recent decades, research about bionic machines has proceeded at a dizzying rate. There have been several significant advances in bionic birds, bionic insects, and bionic fish. Numerous high-quality prototypes have been constructed over time, and a few of them have been adapted for national defense or commercial use. Among them, FWMAVs with a double clap-and-fling mechanism which we usually name it clapping wing micro air vehicles (CWMAVs) have superior flight maneuverability and aerodynamic performance.

For clapping wing micro air vehicles, the force components (including aerodynamic, inertial, elastic, and wing-wing forces) play an important role during the downstroke and upstroke phases. The fluid-solid interaction is an important aspect of the flapping flight in terms of force generation and power consumption. Changing the wing geometry and flapping kinematics parameters is regarded as an effective way to affect forces. The shape parameters have large consequences on the forces generated by flapping wings, such that flying biomechanics often rests on the parametric study of wing geometry.

Flapping-wing propulsion belongs to unsteady aerodynamics, and experiments are seen as an efficient way of inquiry. Nguyen et al. conducted an experimental investigation of wing flexibility for a hovering FlowerFly of several wing configurations with the same shape, area, and weight [3]. Percin et al. employed tomographic particle image velocimetry (PIV) technology to investigate the 3-D flow field and unsteady force experimental investigation using clapping and rotating flat plates [4]. Balta et al. performed experimental investigations of the aerodynamic characteristics due to wing clapping in bio-inspired flying robots [5].

It is essential to develop computational models to simulate the flexible flapping-wing propulsion of CWMAV. Validated computational models can be utilized to evaluate the aerodynamic forces at significantly reduced costs and time. Kruppa's validation test of the Kasper wing is a well-known study that prompted scientists to identify the need for a more in-depth analysis of flexible wings [6]. Deng et al. performed a numerical simulation using an in-house-developed computational fluid dynamics solver. Their computational results provided a quantitative prediction of the unsteady aerodynamics of the flapping-wing micro air vehicle. The formation and evolution of the unsteady vortex were visualized [7]. Tay et al. examined the DelFly Micro and found that increasing the pitch angle increases lift. They also discovered that thrust increases with an increase in spanwise flexibility; chord-wise flexibility increases first and then drops, and simultaneous span and chord alterations proved to be the optimal compromise for increasing generated thrust [8].

Concerning the meshless smoothed particle hydrodynamics (SPH) method [9], more and more biometrics problems can be handled well. Based on the Lagrangian technique, the SPH method divides the continuous medium into particles and solves the governing equations of the fluid on each particle [10], [1], [11]. By combining the SPH with the structural solving model, water impact issues involving free-surface fluid-solid interaction (FSI) have been proven to

*This work was supported by CSC (China Scholarship Council) and Sichuan Science and Technology Program (No. 2020JDJQ0036).

[1]Yanwei Zhang and Zhonglai Wang are with School of Mechanical and Electrical Engineering, University of Electronic Science and Technology of China, Chengdu, 611731, China. 201811040814@std.uestc.edu.cn; wzhonglai@uestc.edu.cn. Corresponding author is Zhonglai Wang, phone: +86 18030743536. wzhonglai@uestc.edu.cn

[2]Saullo Giovani Pereira Castro is with Faculty of Aerospace Engineering, Delft University of Technology, 2629 HS, The Netherlands S.G.P.Castro@tudelft.nl

be solved well by SPH, and issues involving substantial deformations and nonlinear material behavior can also have a premium solution. In addition, the SPH approach has been developed as a potential tool for aeronautical applications, opening up new paths for researching air-solid interactions for aerodynamic issues [12]. Most SPH models do not consider air-solid issues. For the solid part, the finite element method (FEM) has many advantages, so the combination of the FEM and SPH becomes a promising strategy for air-solid interaction problems, especially for the aerodynamic analysis problems faced by CWMAV. In our proposed model, the structural domain representing the clapping wing is modeled using FEM which is proved to be an accurate and efficient method, while the fluid domain is modeled using SPH to handle high-speed flapping and large deformation problems. The developed numerical model allows for direct fluid-solid interaction (FSI) by simultaneously solving the displacement evolution of the SPH particles and the FE nodes, enabling load transfer between the two domains through the penalized contact algorithm.

The parametric study can be exploited to selectively identify key parameters associated with aerodynamic performance. Under the same aspect ratio, different wing shapes bring different lifts. There, a specific wing shape is selected in our work [4]. wingspan and aspect ratio of clapping wings are our concerns for design and optimization. The wingspan in this study ranges from 100 mm to 180 mm. Low aspect ratio wings are not overly sensitive to wind shear, gusts, and roughness. In this paper, the aspect ratio is from 1 to 1.8 to make sure that the leading-edge and trailing-edge vortex surrounding low-aspect-ratio wings has a positive effect on lifting forces [13].

All in all, the novelty of the present paper is twofold: (1) a validated and efficient coupling method based on smoothed particle hydrodynamics method (SPH) with finite element method (FEM) is developed for the three-dimensional flexible clapping wing; (2) a parametric analysis for shape characteristics of CWMAV is proposed to discover high lift mechanism behind flapping-wing propulsion, especially for clapping-wing propulsion.

The remaining paper is organized as follows. Section I describes the problem definition and novelty of the present paper. Section II describes the proposed SPH-FEM method used in this study for the FSI model and validation experiment set-up. Section III presents results and discussions of validation experiment and the parametric study. After that, Section IV concludes the work in this paper and recommendations for future studies.

II. DYNAMIC MODEL AND VALIDATION STUDY

A. The proposed modeling technique

The smooth particle hydrodynamics (SPH) method and the contact algorithm between SPH and FEM are presented here in a brief description. SPH-FEM simulations proposed in this paper are conducted under the open-source project DualSPHysics [14], [15], where the air and solid domains are both defined as discrete particles and solved in a weakly compressible way. An approximation to discrete Lagrangian points can be made. The integral representation of SPH implementation for a smooth quantity, β, for particle i in our model, is with the general form of:

$$\beta_i = \sum_{j\in\Omega} \beta_j W_{i,j} V_j \tag{1}$$

where $j \in \Omega$ represents the set of neighboring particles. The kernel function is represented by $W_{i,j} = W(|\mathbf{x}_{i,j}|, h)$, where $(|\mathbf{x}_{i,j}| = |\mathbf{x}_i - \mathbf{x}_j|)$ denotes temporary position variable and h is the smoothing length. The volume of a neighboring particle j is given by the symbol V_j and $V_j = m_j/\rho_j$, where m_j and ρ_j represents the mass and density of particle j, respectively. The summation approximation implies particle first-order consistency. The spatial gradients are computed by a quintic Wendland kernel [16] employed in this paper:

$$W_{i,j} = \alpha_D (1-2q)^4 (2q+1) for 0 \le q \le 2 \tag{2}$$

where $q = |\mathbf{x}_{i,j}|/h$, and α_D is a normalisation term. For proper value towards CWMAV in this paper, $\alpha_D = 21/(16\pi h^3)$ and $h = 1.2\sqrt{2}d_p$, where d_p is the particle spacing.

The governing equations for a fluid domain are described by the Navier–Stokes equations. The equations of fluid dynamics are based on the fundamental physical laws of conservation (the conservation of mass and momentum):

$$D\rho/Dt + \rho\nabla\cdot\mathbf{u} = 0 \tag{3}$$

$$D\mathbf{u}/Dt = -\frac{1}{\rho}\nabla p + \mathbf{g} + \Gamma \tag{4}$$

where ρ represents the fluid density, $\mathbf{u} = (u, v, w)$ is the velocity vector, p is the fluid pressure, and $\mathbf{g}$ is gravitational acceleration. The material derivative is denoted by D/Dt, while the dissipative stress tensors are denoted by Γ. In the weakly compressible SPH, the continuity, incorporating the δ-SPH density diffusion term of Fourtakas et al. [17], is written as:

$$d\rho_i/dt = \sum_{j\in\Omega} m_j \mathbf{v}_{i,j}\cdot\nabla W_{i,j} + \delta h c_0 \sum_{j\in\Omega} V_j \Psi_{i,j}\cdot\nabla W_{i,j} \tag{5}$$

where $\mathbf{v}_{i,j} = \mathbf{v}_i - \mathbf{v}_j$ and $\nabla W_{i,j}$ is the kernel gradient. The speed of sound c_0 is generally set to $20\sqrt{gh_d}$, where $\sqrt{gh_d}$ is the phase speed in a fluid depth gh_d. Gravitational acceleration is indicated by the symbol $\mathbf{g}$. The δ-SPH coefficient, δ, is assumed to be 0.1 (e.g. Kanehira et al. [18]). The diffusion term which could stabilize the density field from high-frequency oscillations is $\Psi_{i,j}$given by (as in Molteni and Colagrossi [19]):

$$\Psi_{i,j} = 2(\rho_j^D - \rho_i^D)\frac{\mathbf{x}_{i,j}}{|\mathbf{x}_{i,j}|} = 2(\rho_{i,j}^T - \rho_{i,j}^H)\frac{\mathbf{x}_{i,j}}{|\mathbf{x}_{i,j}|} \tag{6}$$

the superscripts D, T, and H, respectively, represent the dynamic, total, and hydrostatic densities. The conservation of mass and momentum equations for weakly compressible SPH is given under the Tait equation of state:

$$p = \frac{c_0^2\rho_0}{\gamma}[(\frac{\rho}{\rho_0})^\gamma - 1] \tag{7}$$

where $\rho_0 = 1.29kg/m^3$ is set to the reference density of air for CWMAV, and $\gamma = 7$ is the polytropic index. Equation (7) is an extremely stiff equation because its combination with particle disorder may produce problems of large non-physical density fluctuations. To reduce these instabilities and distributions, we consequently incorporate the δ-SPH density diffusion factor in (5) to smooth most of the high-frequency oscillations. The momentum equation, laminar viscosity, and sub-particle scale (SPS) turbulence are given by:

$$(\mu\nabla^2\mathbf{v})_i = \sum_{j\in\Omega} m_j\left(\frac{4\mu|\mathbf{x}_{i,j}|\cdot\nabla W_{i,j}}{(\rho_i+\rho_j)(x_{i,j}^2+0.001h^2)}\right) \quad (8)$$

where μ is kinematic viscosity, which is set to 0.0000148 in our model, this treatment can avoid numerical unnecessary instabilities without leading to over diffusive [20].

B. A parametric study

Fig. 2 presents the physical model of the designed CW-MAV in this work, whose clapping wing is made of polyethylene (PE) film and carbon fiber reinforced polymer (CFRP) rod, with the weight being able to reach around 17g. The flapping wing with a double clap-fling mechanism is our research focus in this work. To independently analyze the influence of wing shape parameters on aerodynamic characteristics, we only model the clapping wing and specify the motion mode. A parametric study is carried out to analyze the effect of the wingspan on the responses of the aerodynamic forces, which is the subject of this paper.

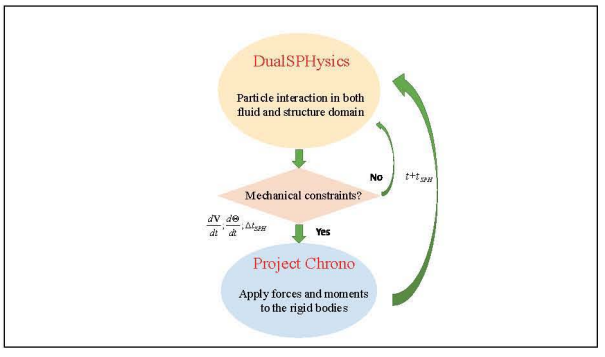

Fig. 1. Contact algorithm for fluid-solid interaction

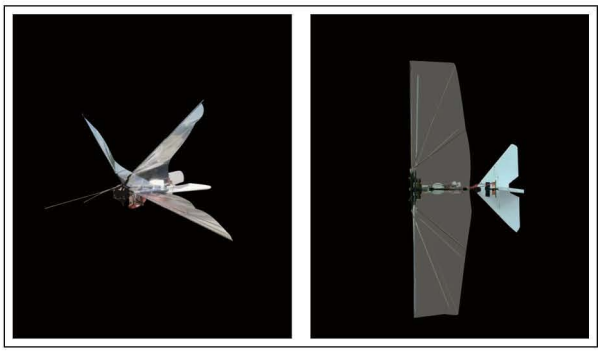

Fig. 2. The physical model of CWMAV

A summary of the parameters utilized in our numerical model is described in this section. The flow field is a cuboid with dimensions of 0.8 m × 1 m × 0.2 m. A novel presentation form is proposed to reconduct the veins of CWMAV. Fig. 3(b) is a numerical modelling inspiration of experimental wings (Fig. 3(a)). As a result, a quasi-flexible wing is proposed by substituting spring connections for the obliquely placed carbon rods. The figure also shows that the wing is orderly divided into six parts by ball links between the wing root and the leading edge (the black circle) and linear springs at another end of the vein (the yellow circle). For the wing's materials, the Young module is set to 69 MPa, the Poisson ratio is 0.3, the restitution coefficient is 0.001, and the coefficient of friction of 0.45. By adjusting the stiffness and damping values of the links, we could control the quasi-flexible condition of the clapping wing. The simulated flexibility of the flapping wing can be observed in Fig. 4. This treatment expands the application of the SPH-FEM method in handling flexible bodies.

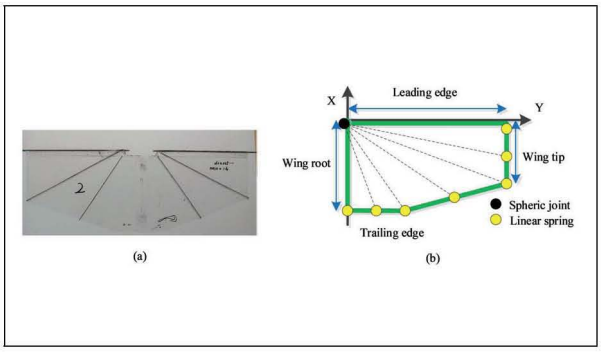

Fig. 3. The physical and simulated wing

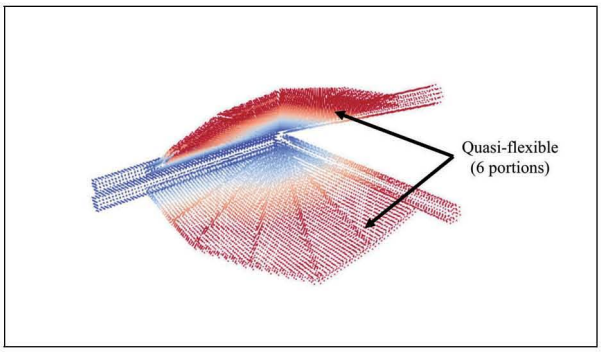

Fig. 4. The quasi-flexible clapping wings

In all cases, the clapping wing is subjected to a flight attitude with the flapping frequency of 12 Hz, angle of attack of 15 degrees, flapping amplitude of 75 degrees, and wind velocity of 3.5 m/s for each wingspan level for several periods [4]. To figure out the aerodynamic characteristics of the specific layout wings, five levels of wingspan are selected: 100, 120, 140, 160, 180 mm at the same chord length of 90 mm (aspect ratio: 1.1, 1.3, 1.5, and 1.9). The wingspan of the trailing edge is also adjusted proportionally: 47, 56, 65, 74, and 83 mm, respectively.

$$(\mu\nabla^2\mathbf{v})_i = \sum_{j\in\Omega} m_j\left(\frac{4\mu|\mathbf{x}_{i,j}|\cdot\nabla W_{i,j}}{(\rho_i+\rho_j)(x_{i,j}^2+0.001h^2)}\right) \quad (8)$$

C. Validation study

A validation experiment is presented where the proposed method is used to calculate lift for comparison. Our platform consists of a test model, a clamping regulator, a wind tunnel, a mechanical data acquisition system, a PIV system, and a synchronizer system. The test model comprises a clapping wing configuration made of PE film and reinforced with carbon rods as veins. The wingspan of each wing is chosen to be 140 mm and the weight is 17 g. The experiments are carried out in a low-speed wind tunnel whose set-up is presented in Table I

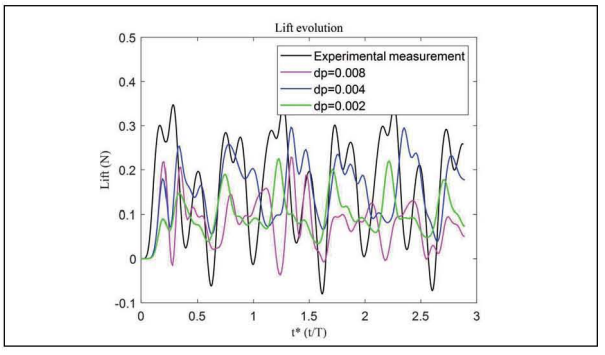

Fig. 5. The difference between experimental measurements and SPH-FEM measurements

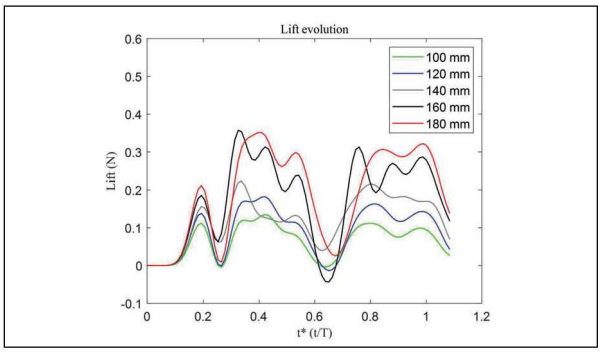

Fig. 6. Comparison of lift history for flapping wings with different wingspan

III. RESULTS AND DISCUSSIONS

A. Validation results

The validation study is done with the help of the mechanical measurement component of our PIV platform. Three particle spacings d_p of proposed numerical model d_p are selected: 0.008 m, 0.004 m, and 0.002 m. Fig. 5 illustrates that a good fit is seen between the experiment and calculated values for various d_p values as represented by lift evolutions. A low-pass filter and a reduction of inertial forces are implemented for data analysis. The comparison of lift history in Fig. 5 shows that situations with $d_p = 0.004$ m and $d_p = 0.002$ m have a more similar trend and magnitude to the experimental force. Moreover, comparative analysis shows that setting $d_p = 0.002$ m results in an excessively time-consuming model considering particles of simulation. Thus, to strike a balance between sufficient precision and computational expense, a magnitude of $d_p = 0.004$ m is adopted for parametric study in this work.

TABLE I

EXPERIMENTAL SET-UP FOR VALIDATION STUDY

Devices	Parameters
Low-speed tunnel	1.2 m 1.2 m, 0-30 m/s
Mechanical sensor	ATI-Nano 17
Measurement accuracy	$F_x, F_y = 8$ N, $F_z = 14$ N, $M_x, M_y, M_z = 0.005$ Nm, 1/160 N
Mechanical data acquisition card	National Instruments, NI
High-speed camera	85 mm, 8000 Hz, 1024×1024 pixels, Phantom 7.3, TRI America
High-frequency laser	532 , 200 mJ, 2560×2160 pixels, ILA Germany
Frequency senor	0-50 Hz7

B. Parametric study

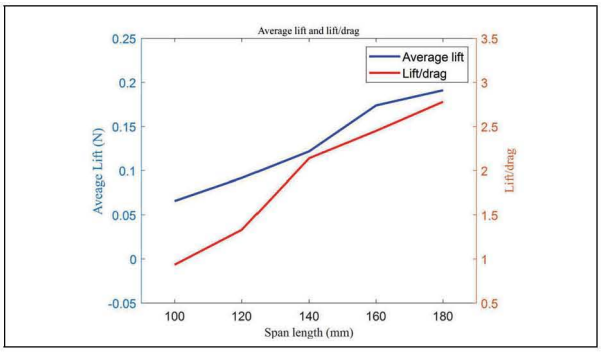

Fig. 7. Comparsion of average lift and lift/drag with different wingspan

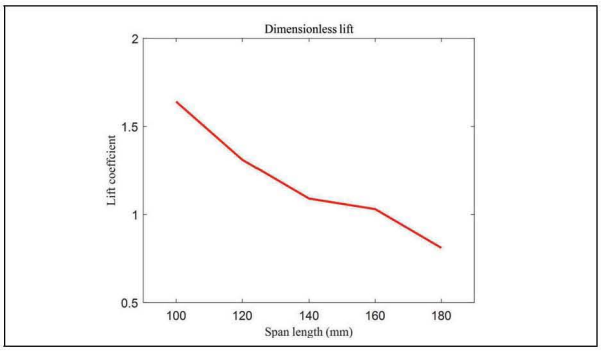

Fig. 8. Comparsion of lift coefficient with different wingspan

In this section, discussions on wingspan impact investigation on the lift will be presented. As detailed in Section II, different parameters are considered in this work: 100, 120, 140, 160, 180 mm at the same chord length of 90 mm (aspect ratio: 1.1, 1.3, 1.5, and 1.9). Evolution and period-average lift contributed by clapping wings are considered as the level of aerodynamic performance. And finally, the results of this parametric study are discussed.

Fig. 6 presents the lift evolution for these five cases where clap-fling motion begins at the start of the out-stroke phase. The time history curves are numerically integrated to obtain the characteristics and it can be observed from the quantitative comparison the lift peak increases with wingspan. The peaks in the lift evolution are largest with a wingspan of 180 mm and further reduce slightly in the decrease of wingspan. For instance, the maximum lift peak is around 0.35 N, which

drops to 0.22 N for a wingspan of 140 mm. Further, the trend does not change with different wingspans. Also, the lift amplitude increases with the wingspan.

Fig. 7 compares the period-average lift and lift/drag for all cases. It can be seen from the figure that the wingspan has a positive effect on average lift and lift/drag. Also, the results clearly show that the lift/drag ratio is dominated by the wingspan. The largest average lift and lift/drag are with a wingspan of 180 mm. There is no doubt that the wingspan under this type of wing shape brings higher lift.

Further, to have a deep understanding of the effects of wingspan, the lift coefficient (a dimensional variable) is discussed in Fig. 8.

$$C_L = \frac{L}{\rho U_{tip}^2 S} \tag{9}$$

where C_L is the lift coefficient, U_{tip} represents average wingtip velocity, and S is the Wing surface area. It is found that the lift coefficient declines rapidly with the increase in the wingspan.

IV. CONCLUSIONS

This study investigates the aerodynamic characteristics of a clapping wing micro air vehicle by a novel air-solid interaction model. In the air domain, the SPH method is applied to calculate particle interaction. In the solid domain, the FEM method undertakes the tasks of forces and moments application. Besides, a quasi-flexible modeling method is adopted to restore the flexibility of clapping wings. To verify the accuracy of our numerical model, a physical prototype is designed and tested in this work. The results obtained from our numerical study are in satisfactory agreement with the experimental study. Based on the built aerodynamic model, the wingspan is discussed under a parametric study. The obtained results show that wingspan has a basically positive effect on lift and lift/drag, but it brings a decrease in lift coefficient. Our study provides a better understanding of the unsteady mechanism of CWMAV. Future work will extend this parametric study and develop a design and optimization model for CWMAV, further to achieve nimble flapping flight.

ACKNOWLEDGMENT

This work was funded by CSC (China Scholarship Council) and Sichuan Science and Technology Program (No. 2020JDJQ0036).

REFERENCES

[1] M. Ellero, M. Serrano, and P. Español, "Incompressible smoothed particle hydrodynamics," *Journal of Computational Physics*, no. 2, pp. 1731–1752, oct 2007.

[2] M. A. Fenelon, "Biomimetic flapping wing aerial vehicle," in *2008 IEEE International Conference on Robotics and Biomimetics*. IEEE, 2009, pp. 1053–1058.

[3] Q. V. Nguyen, W. L. Chan, and M. Debiasi, "Experimental investigation of wing flexibility on force generation of a hovering flapping wing micro air vehicle with double wing clap-and-fling effects," *International Journal of Micro Air Vehicles*, vol. 9, no. 3, pp. 187–197, 2017.

[4] M. Percin, B. W. van Oudheusden, G. C. H. E. de Croon, and B. Remes, "Force generation and wing deformation characteristics of a flapping-wing micro air vehicle 'DelFly II' in hovering flight," *Bioinspiration & Biomimetics*, vol. 11, no. 3, p. 036014, may 2016.

[5] M. Balta, D. Deb, and H. E. Taha, "Flow visualization and force measurement of the clapping effect in bio-inspired flying robots," *Bioinspiration & Biomimetics*, vol. 16, no. 6, p. 066020, 2021.

[6] E. W. Kruppa, "A wind tunnel investigation of the Kasper vortex concept," in *13th Annual Meeting and Technical Display Incorporating the Forum on the Future of Air Transportation*. Reston, Virigina: American Institute of Aeronautics and Astronautics, jan 1977.

[7] S. Deng, M. Percin, and B. van Oudheusden, "Aerodynamic characterization of 'delfly micro'in forward flight configuration by force measurements and flow field visualization," *Procedia Engineering*, vol. 99, pp. 925–929, 2015.

[8] W. Tay, B. van Oudheusden, and H. Bijl, "Numerical simulation of a flapping four-wing micro-aerial vehicle," *Journal of Fluids and Structures*, vol. 55, pp. 237–261, may 2015.

[9] J. J. Monaghan, "Smoothed Particle Hydrodynamics," *Annual Review of Astronomy and Astrophysics*, vol. 30, no. 1, pp. 543–574, sep 1992.

[10] S. Shao and E. Y. Lo, "Incompressible SPH method for simulating Newtonian and non-Newtonian flows with a free surface," *Advances in Water Resources*, vol. 26, no. 7, pp. 787–800, jul 2003.

[11] P. Nair and G. Tomar, "An improved free surface modeling for incompressible SPH," *Computers & Fluids*, vol. 102, pp. 304–314, oct 2014.

[12] B. Ren, X. Yan, T. Yang, C.-f. Li, M. C. Lin, and S.-m. Hu, "Fast SPH simulation for gaseous fluids," *The Visual Computer*, vol. 32, no. 4, pp. 523–534, apr 2016.

[13] G. E. Torres and T. J. Mueller, "Low aspect ratio aerodynamics at low reynolds numbers," *AIAA journal*, vol. 42, no. 5, pp. 865–873, 2004.

[14] A. Crespo, J. Domínguez, B. Rogers, M. Gómez-Gesteira, S. Longshaw, R. Canelas, R. Vacondio, A. Barreiro, and O. García-Feal, "DualSPHysics: Open-source parallel CFD solver based on Smoothed Particle Hydrodynamics (SPH)," *Computer Physics Communications*, vol. 187, pp. 204–216, feb 2015.

[15] J. M. Domínguez, G. Fourtakas, C. Altomare, R. B. Canelas, A. Tafuni, O. García-Feal, I. Martínez-Estévez, A. Mokos, R. Vacondio, A. J. C. Crespo, B. D. Rogers, P. K. Stansby, and M. Gómez-Gesteira, "DualSPHysics: from fluid dynamics to multiphysics problems," *Computational Particle Mechanics*, mar 2021.

[16] H. Wendland, "Piecewise polynomial, positive definite and compactly supported radial functions of minimal degree," *Advances in Computational Mathematics*, vol. 4, no. 1, pp. 389–396, dec 1995.

[17] G. Fourtakas, J. M. Dominguez, R. Vacondio, and B. D. Rogers, "Local uniform stencil (lust) boundary condition for arbitrary 3-d boundaries in parallel smoothed particle hydrodynamics (sph) models," *Computers Fluids*, vol. 190, pp. 346–361, 8 2019.

[18] T. Kanehira, H. Mutsuda, S. Draycott, N. Taniguchi, T. Nakashima, Y. Doi, and D. Ingram, "Numerical re-creation of multi-directional waves in a circular basin using a particle based method," *Ocean Engineering*, vol. 209, p. 107446, aug 2020.

[19] D. Molteni and A. Colagrossi, "A simple procedure to improve the pressure evaluation in hydrodynamic context using the SPH," *Computer Physics Communications*, vol. 180, no. 6, pp. 861–872, jun 2009.

[20] R. Canelas, M. Brito, O. Feal, J. Domínguez, and A. Crespo, "Extending DualSPHysics with a Differential Variational Inequality: modeling fluid-mechanism interaction," *Applied Ocean Research*, vol. 76, pp. 88–97, jul 2018.